ELSEVIER

Ceramics International 27 (2001) 443–449

CERAMICS INTERNATIONAL

www.elsevier.com/locate/ceramint

In situ co-textured microstructure of alumina/alumina: Ca-hexaluminate multilayer composites

Jun-Ho Song, Sang-Yeup Park *

Department of Ceramics Engineering, Kangnung National University, Kangnung, Kangwondo 210-702, South Korea

Received 3 July 2000; received in revised form 17 July 2000; accepted 30 August 2000

Abstract

In situ co-textured microstructure of alumina/alumina:Ca-hexaluminate multilayer composites has been investigated. Ca-hexaluminates, in situ grown in the presence of $CaMgSiO_4$ glass, showed a well-textured microstructure in Ca-hexaluminate/alumina multilayer composites. In situ texturing of Ca-hexaluminate was possible through the microstructure texturing of alumina using alumina platelets and $CaMgSiO_4$ glass. $CaMgSiO_4$ glass addition was effective for the in situ texturing of Ca-hexaluminates as well as the microstructure texturing of alumina. The in situ textured Ca-hexaluminate and alumina multilayer composites provide a well-controlled crack propagation because of crack shielding and crack deflection. © 2001 Published by Elsevier Science Ltd and Techna S.r.l. All rights reserved.

Keywords: In situ texturing; Alumina/alumina: Ca-hexaluminate; Multilayer composites

1. Introduction

The microstructure texturing concept has been gaining attention in the processing of ceramics materials with anisotropic grain morphology [1–3]. Compared to the traditional processing of a fine and equiaxed microstructure, textured microstructures with anisotropic grain are expected to enhance structural and electronic properties. Messing et al. [2] have been developed a well textured microstructure of Al_2O_3 and mullite by combining seeding and anisotropic grain growth in the presence of a liquid phase. As a typical example of anisotropic growth, β-Si_3N_4 with high toughness has been achieved for in situ toughened Si_3N_4 compared to a fine grained Si_3N_4 [4]. As a closely analogus concept to in situ toughened materials, Chen and Chen [5] studied the mechanical behavior of various hexaluminates reinforced alumina composites ($LaAl_{11}O_{18}$, $LaMgAl_{11}O_{19}$, $SrAl_{12}O_{19}$, $CaAl_{12}O_{19}$ and $Na_2MgAl_{12}O_{17}$) based on in situ growth of hexaluminate. In their works, improved fracture toughness has been achieved because of crack bridging by the hexaluminates.

Ca-hexaluminate ($CaAl_{12}O_{19}$ or CA_6) with a magnetoplumbite structure is known to enhance the damage tolerance of oxide composites without any degradation of strength [6]. Ca-hexaluminate is composed of spinel blocks and mirror planes stacked alternatively along the c-axis, and large alkali ions are easily accommodated in mirror planes known to be mechanically weak [7]. Because this compound is expected to be used as a candidate material for a weak interface, several studies have been made upon the effect of Ca-hexaluminate based on in situ toughening of alumina composites [6,8]. Now the in situ toughening concept using Ca-hexaluminate has been extended to trilayer composites with heterogeneous microstructure in order to improve the capability of crack suppression and wear resistance [9].

In this study, it was attempted to design the heterogeneous multilayer composites consisting of a homogeneous layer with untextured alumina and a heterogeneous layer with co-textured alumina and Ca-hexaluminate. There are two reasons for the selection of this system. Firstly, the in situ co-texturing of CA_6 may be possible through in situ anisotropic growth during the microstructure texturing of alumina which was demonstrated in a previous study [2]. Secondly, the presence of in situ co-textured CA_6 in textured alumina may provide a profound influence on the crack propagation.

* Corresponding author. Tel.: +82-391-640-2363; fax: +82-391-640-2244.

E-mail address: sypark@knusun.kangnung.ac.kr (S.-Y. Park).

0272-8842/01/$ - see front matter
PII: S0272-8842(00)00099-7

2. Experimental

Starting powder was α-Al_2O_3 (AKP-50, Sumitomo Chemical, Japan) with 0.3 μm and 99.999% purity. As a template for the texturing alumina, α-alumina platelet (AL-13PCA, Showha Electric, Japan) 40 μm in size and 1 μm in thickness and 99.8% purity were used in this experiment. $CaMgSiO_4$ (monticellite) glass was prepared with $CaCO_3$, MgO, SiO_2, and Al_2O_3 of reagent grade.

Stable aqueous slips of Al_2O_3 with 50 vol.% of solid loading were prepared by adjusting the pH value (=8.5) with NaOH. For a good dispersion, the total amount of 2.5 wt.% polyglycerol, cellulose, and silicon emulsion were added to enhance the powder dispersion. It was then ball-milled for 24 h in a polyethylene jar using a Si_3N_4 ball. After ball-milling, the slurry was ultrasonically treated to remove the soft agglomerate.

Green laminates were prepared by continuous slip casting with a dimension of 40 × 40 mm. Alumina/alumina:Ca-hexaluminate laminates were fabricated by alternating layers (total 21 layers) of alumina of 50 μm thickness and alumina-5 vol.% $CaMgSiO_4$ (CMS) glass layer of 50 μm thickness. In the specimen notation, A means alumina layer and A–AP means alumina platelet added alumina layer, and A–AP–CMS means alumina platelet and $CaMgSiO_4$ glass added alumina layer. Green laminates were dried in air and then calcinated at 700°C for 2 h. Samples were pressureless sintered between 1600 and 1650°C for 16 h.

Thermogravimetric analysis (TGA) was performed on the specimen with a constant heating rate of 10°C/min.

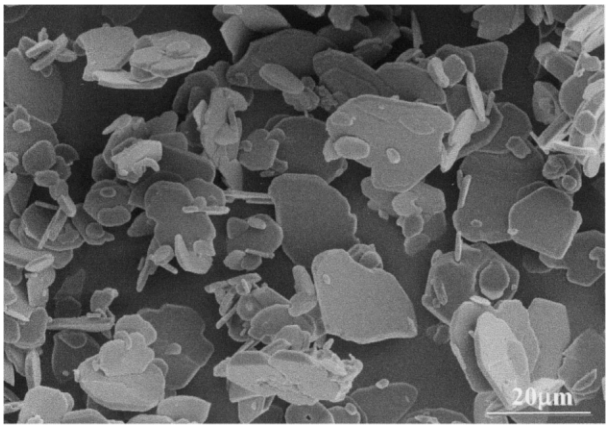

Fig. 1. SEM micrograph of α-Al_2O_3 platelets.

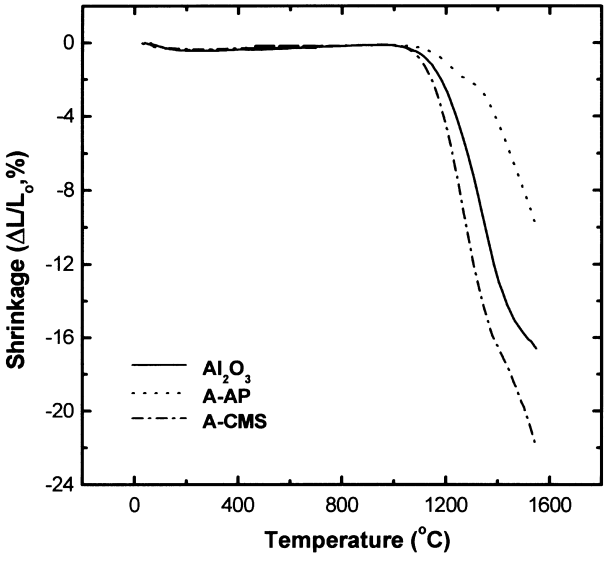

Fig. 2. Change of shrinkage with temperature.

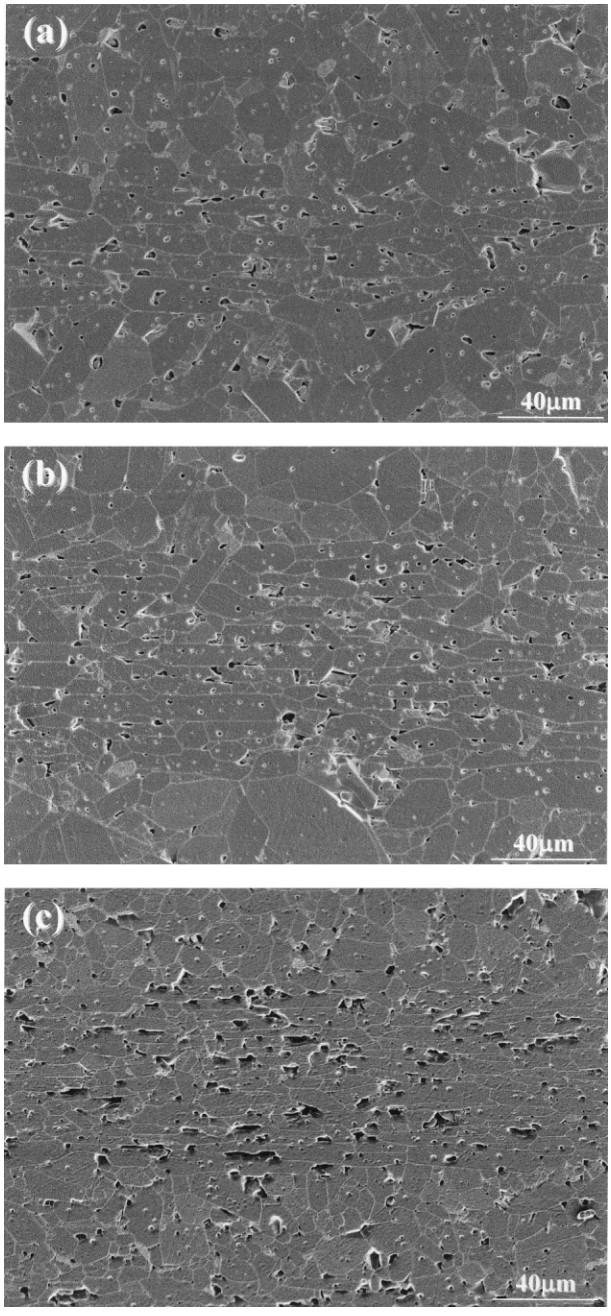

Fig. 3. SEM micrographs of thermally etched A–AP samples; (a) 5 vol.% platelets, (b) 10 vol.% platelets, and (c) 15 vol.% platelets.

Dilatometer measurement was carried out in order to measure the shrinkage rate of the laminates. Specimens were polished with a diamond slurry and then thermally etched in order to reveal the microstructure. Vicker's indentation cracks were generated under a 10 kg load on the polished surface of specimen in order to observe the crack propagation behavior. The polished specimens were thermally etched and then the microstructure was observed using scanning electron microscopy (SEM). Average grain size and orientation angle were determined by measuring each grain using an image analyzer. Approximately 400 grains were measured for each sample. The degree of texturing was determined by XRD using Cu-K_α radiation. Energy dispersive X-ray spectrometry (EDS) analysis was performed to confirm the formation of Ca-hexaluminate.

3. Results and discussion

Fig. 1 shows the α-alumina platelets used as the template in this study. Based on TGA measurement of a green specimen, organic components such as binder and dispersant were burned-out below 400°C, and there was no more weight loss above 400°C. Based on the TGA results, green laminates were calcined at 700°C for 2 h. Fig. 2 shows dilatometer results as a function of temperature. Shrinkage was started from 1000°C and the A–CMS specimen showed a relatively large shrinkage compared to the alumina and A–AP specimens. Among those specimens, A–AP showed a relatively small shrinkage compared to alumina. These results suggest that the addition of CMS glass was effective for the

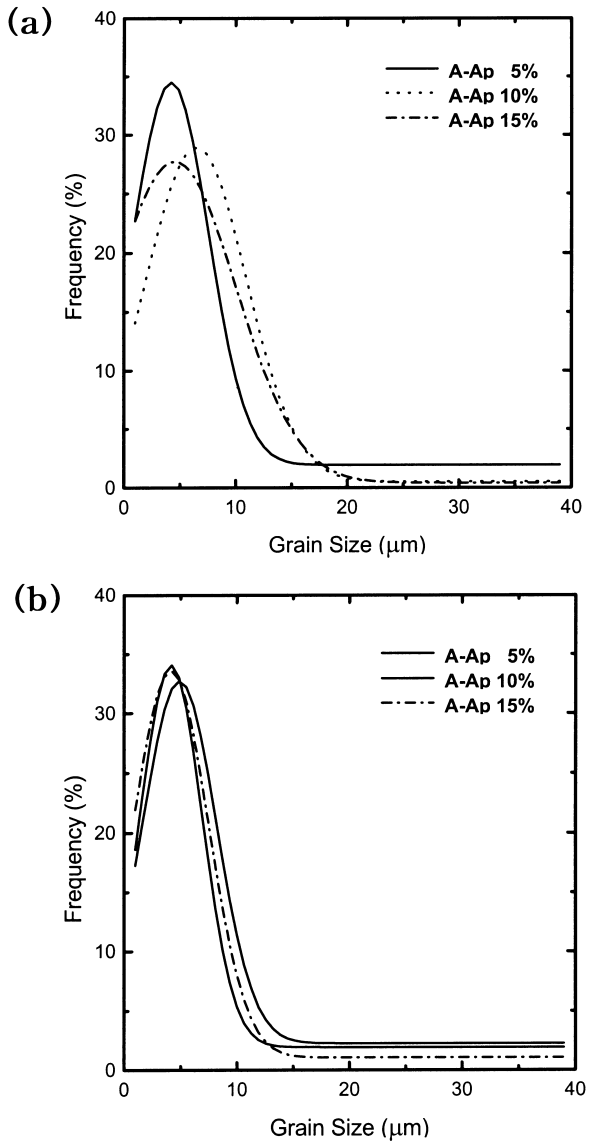

Fig. 4. Grain size distribution of alumina in (a) textured and (b) untextured layer. Specimens were sintered at 1600°C for 16 h.

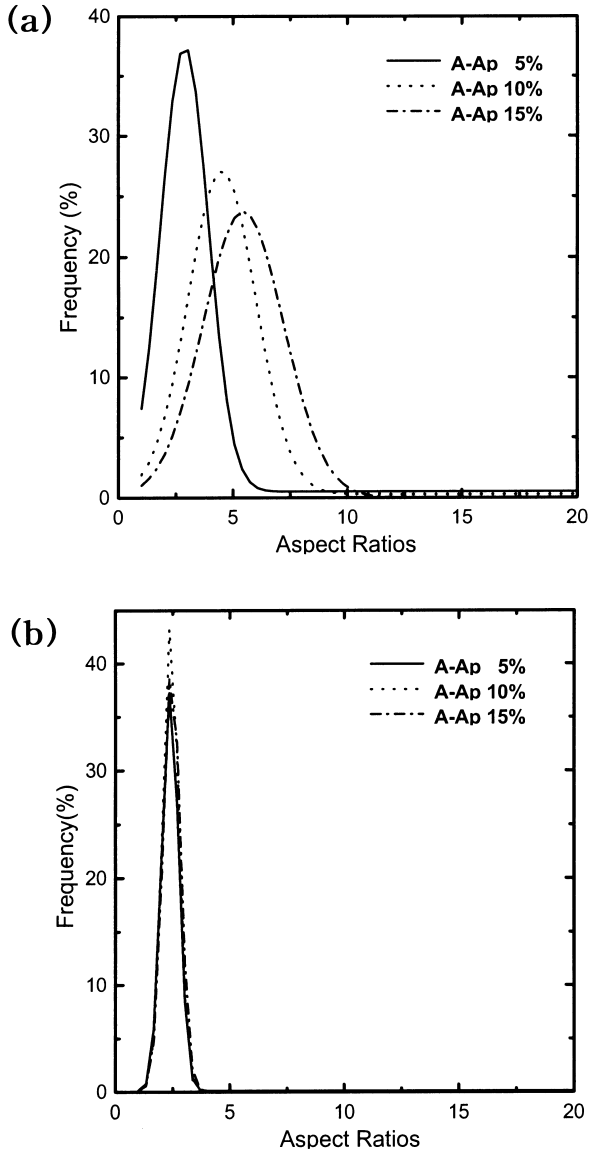

Fig. 5. Aspect ratios of alumina in (a) textured and (b) untextured layer. Specimens were sintered at 1600°C for 16 h.

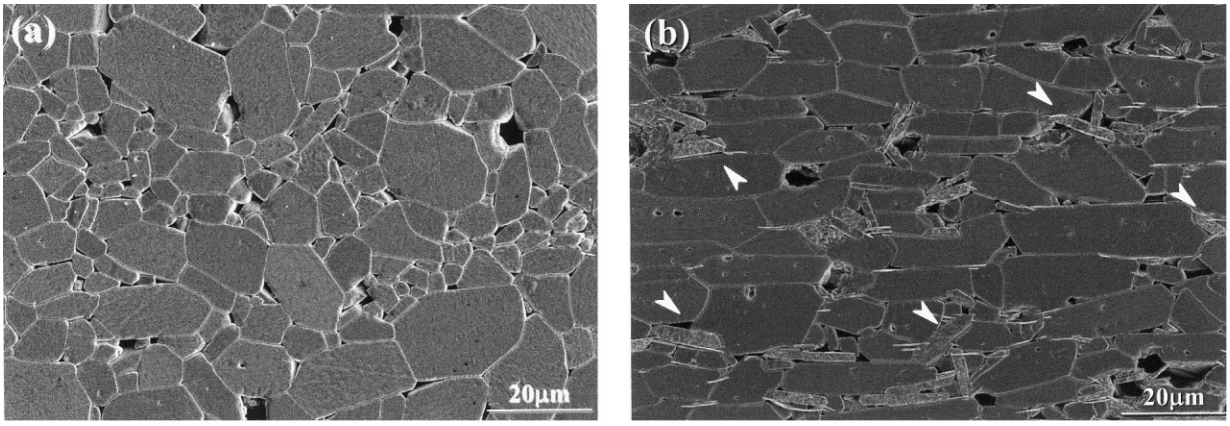

Fig. 6. SEM micrograph of untextured alumina (a) and in situ co-textured microstructure composed of alumina and Ca-hexaluminate (b) in the specimen with CMS glass, sintered at 1600°C for 16 h.

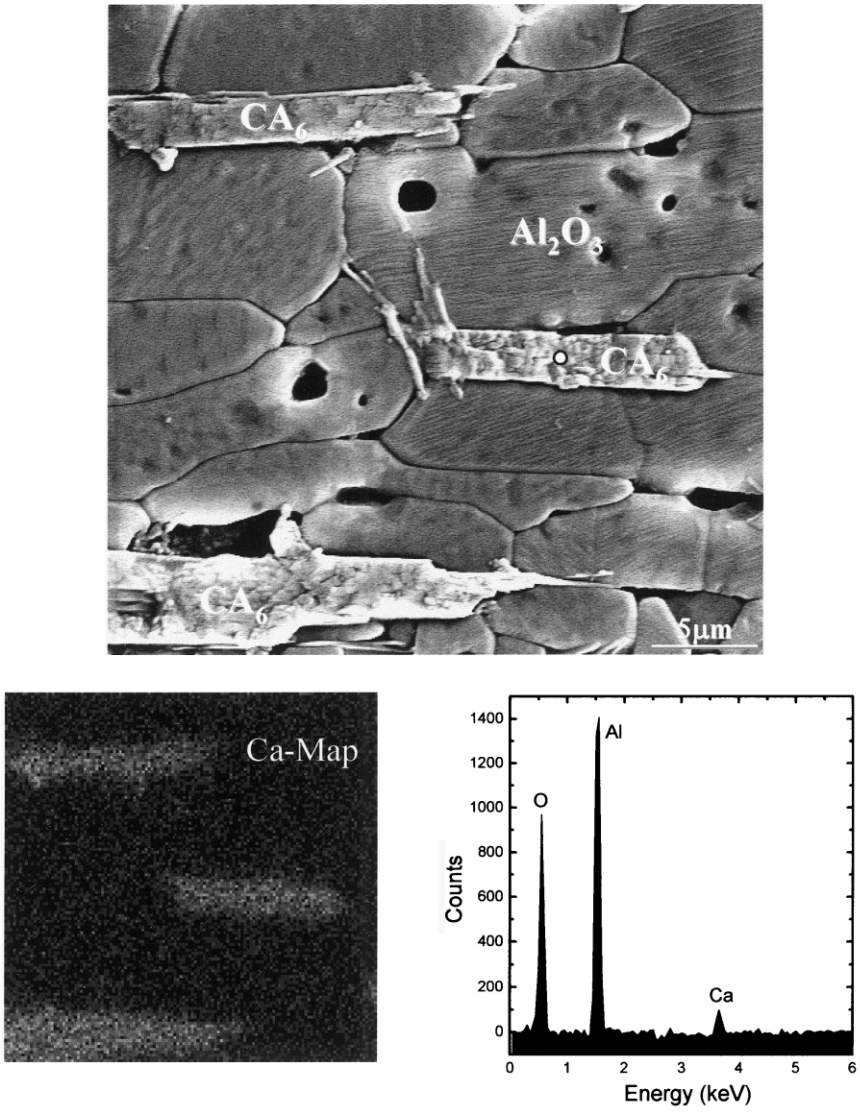

Fig. 7. EDS analysis of CA_6 grains in a textured layer.

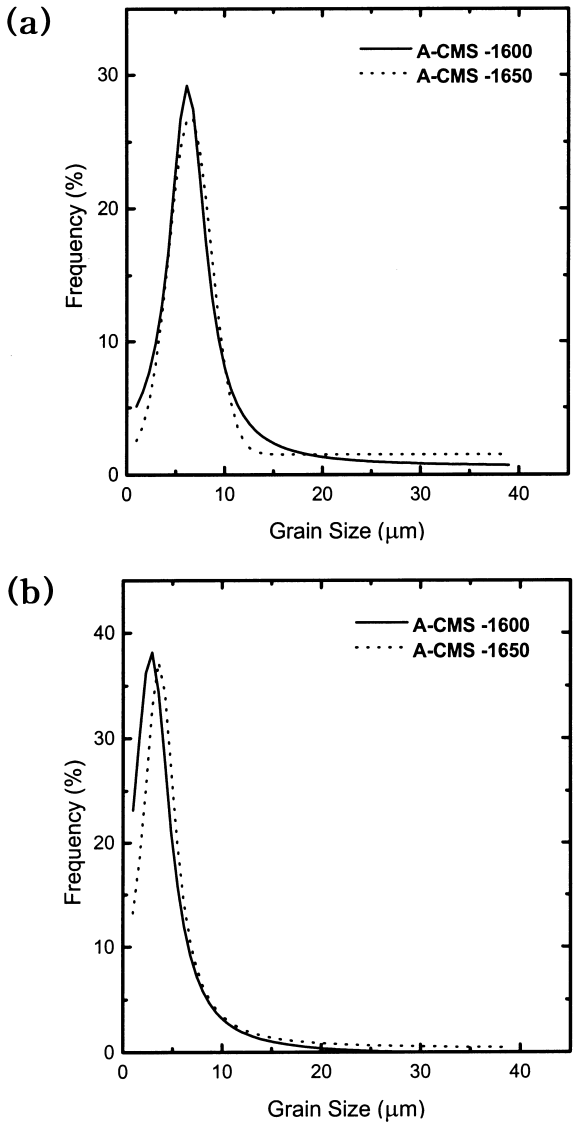

Fig. 8. Grain size distribution of alumina in (a) textured and (b) untextured layer. Specimens were sintered at 1600°C for 16 h.

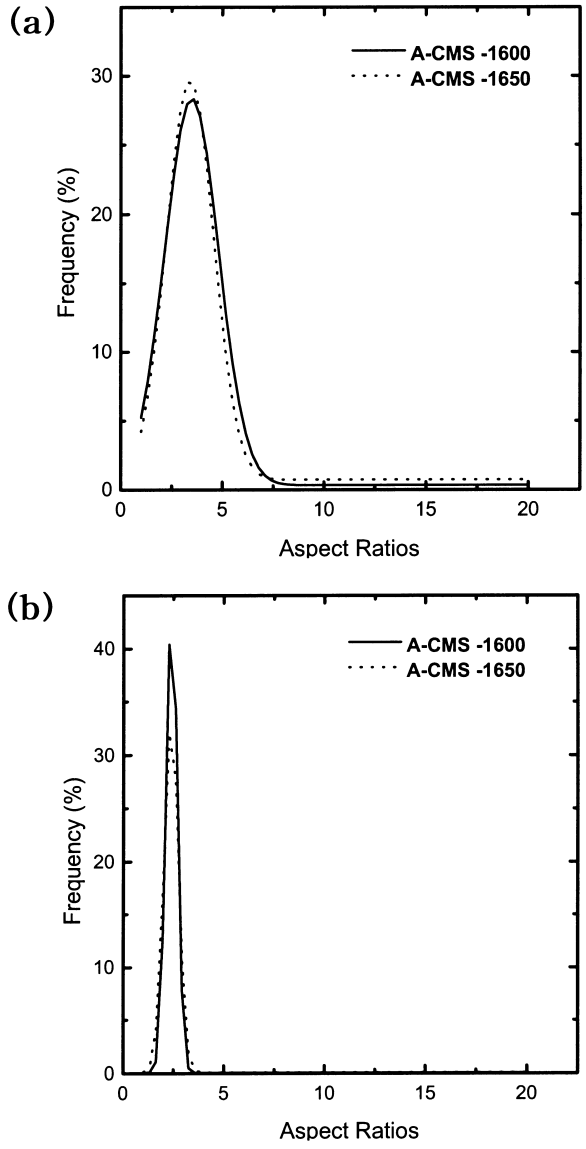

Fig. 9. Aspect ratios of alumina in (a) textured and (b) untextured layer. Specimens were sintered at 1600°C for 16 h.

densification of laminate because of the formation of a liquid phase.

Fig. 3 shows the effect of platelet loading on the textured microstructure of alumina. In the case of platelet addition, alumina grains were aligned towards the casting direction in the textured layer, whereas alumina grains exhibited random growth in the untextured layer. With increasing the platelet loading up to 15 vol.%, porosity was increased and pore shape was changed from spherical to faceted due to the impingement of platelets during grain growth. Although abnormal grains were observed in the untextured alumina layer, abnormal grain growth in the untextured layer can be reduced substantially with the addition of MgO doping (0.1 wt.%).

Fig. 4 shows grain size distribution with an increase in the platelet content both in the textured and untextured layers. With an increase in the platelet loading, grain size distribution was widen in the textured layer. However, grain size distribution remained nearly constant regardless of platelet loading. In addition, the aspect ratios distribution of alumina exhibited the same tendency as the grain size distribution, as shown in Fig. 5. With an increase in the sintering time and temperature, platelets continue to grow in the thickness-direction rather than length-direction because of the impingement of each anisotropic grain.

Fig. 6 shows SEM microstructure composed of textured alumina and anisotropic grains in the specimen with CMS glass. Anisotropic grains were well-aligned between alumina grains. From the EDS analysis, the chemical composition of anisotropic grains was identified as Ca-hexaluminate with stoichiomeric composition

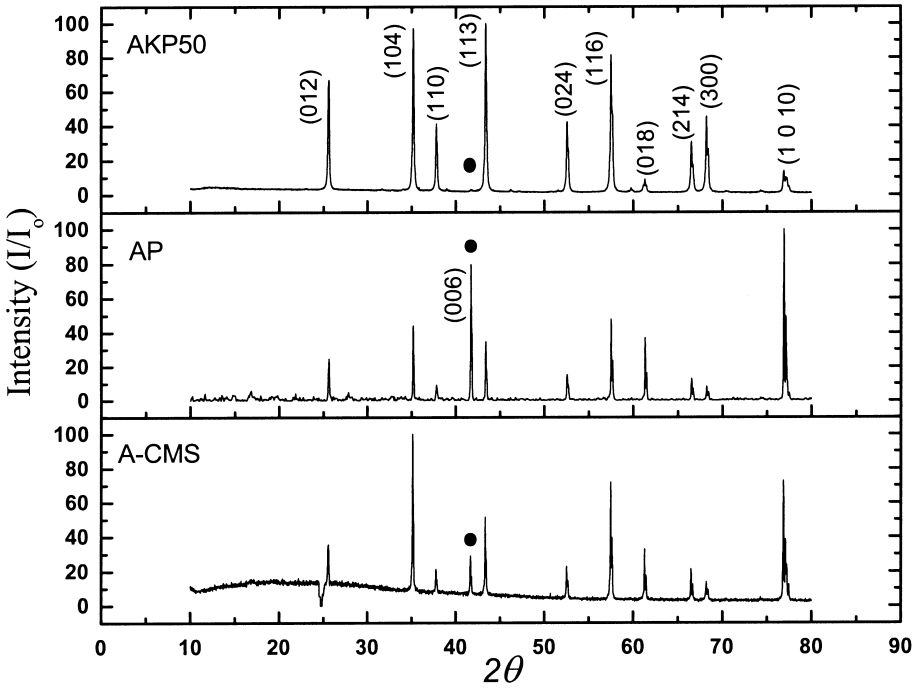

Fig. 10. XRD patterns showing the intensity difference.

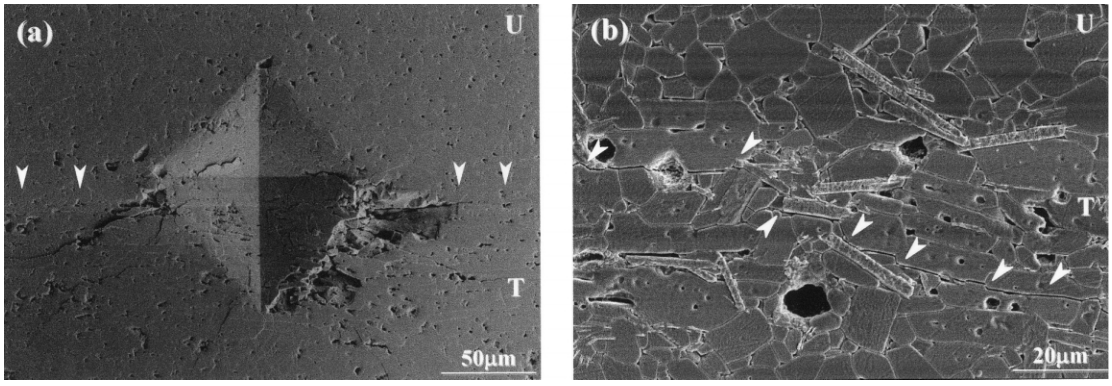

Fig. 11. SEM micrographs of A-CMS system showing (a) Vicker's indentation pattern and (b) crack propagation behavior with 10 kg load in alumina/alumina:CA_6 multilayer composites; U indicates untextured layer and T indicates textured layer.

(Ca/Al = 1/12). The anisotropic morphology of CA_6 grains can be clearly observed in the Ca-map, as shown in Fig. 7. In this case, the formation of CA_6 with platelet shape might be influenced by the Ca rich liquid phase, for example solution reprecipitation reaction between Ca-monoaluminate ($CaAl_2O_4$ or CA) and alumina [10]. Considering the small grain size of CA_6 compared to textured alumina grain, it is believed that the nucleation of the CA_6 grain after the texturing process of alumina resulted in a co-textured microstructure.

It has been reported that the morphology of CA_6 changed from an elongated shape to an equiaxed shape in the presence of a small concentration of Mg^{2+} ion [10]. In our study, however, the morphology of CA_6 grains retained elongated shapes without any morphology change in the presence of a suitable concentration of Mg^{2+}. Thus, the authors believe that Mg^{2+} does not severely suppress the anisotropic grain growth of CA_6 in a relatively sufficient amount of the liquid phase. Fig. 8 shows the grain size distribution of alumina in A–CMS system. The grain size distribution of alumina exhibited a relatively wide distribution in the untextured layer compared to the textured layer. Also, aspect ratios of alumina grain showed a similar tendency as the grain size distribution, as shown in Fig. 9. Such a wide distribution both in grain size and in aspect ratios indicates that a strong texturing of alumina was developed in the layer containing alumina and CA_6.

XRD measurements were performed on the textured layers perpendicular to the stacking direction. XRD patterns of textured alumina are shown in Fig. 10. Compared with the untextured layer, for example alu-

mina powder, the strong intensity of alumina peaks both in the (006) plane and in the (1010) plane was observed in textured layers. The peak intensity of (006) plane in A–CMS specimen was relatively weak compared to A–AP specimen. This intensity difference resulted from the formation of the CA_6 phase during sintering. From the XRD patterns and SEM micrographs, it is clear that the addition of alumina platelets provide a nucleation site for textured alumina.

Crack propagation behavior of alumina laminate composites is shown in Fig. 11. After indentation on the polished surface with a 10 kg load, damage pattern revealed a different one [Fig. 11(a)] compared to the typical indentation pattern showing a straight crack propagation at the indenter's corner. Such a diffuse damage pattern, indicating shear fault resulting from a weak interface has been reported in platelet reinforced composites [9]. When the cracks entered the co-textured layer, cracks were deflected at the interface between CA_6 and alumina and crack bridging was observed, as shown in Fig. 11(b). Because Ca-hexaluminate is known to form a weak interface in the alumina matrix [6], indentation damage could be dissipated by the crack shielding effect at the CA_6 interface. Thus, it is believed that alumina/alumina:CA_6 multilayer composites provide more enhanced crack arrestment compared to trilayer composites from the consideration of in situ co-textured CA_6 in alumina matrix.

4. Conclusions

In situ microstructure texturing of alumina/alumina:Ca-hexaluminate multilayer composites total 21 layers has been investigated using the continuous slip casting method. Ca-hexaluminates, in situ grown in the presence of $CaMaSiO_4$ glass, showed a well-textured microstructure in Ca-hexaluminate/alumina multilayer composites. Such an in situ texturing of Ca-hexaluminate was possible through the microstructure texturing of alumina using alumina platelets and $CaMgSiO_4$ glass. $CaMgSiO_4$ glass was effective for the in situ texturing of Ca-hexaluminates as well as the microstructure texturing of alumina. The in situ co-textured Ca-hexaluminate and alumina multilayer composites provide a well-controlled crack propagation and crack shielding behavior.

References

[1] D. Brandon, D. Chen, H.M. Chan, Control of texturing in monolithic alumina, Mater. Sci. Eng. A195 (1995) 189.
[2] M.M. Seabaugh, I.H. Kerscht, G.L. Messing, Texturing development by templated grain growth in liquid phase sintered α-alumina, J. Am. Ceram. Soc. 80 (5) (1997) 1181.
[3] L. An, Indentation fatigue in random and textured alumina composites, J. Am. Ceram. Soc. 82 (1) (1999) 178.
[4] A.J. Pysik, D.R. Beaman, Microstructure and properties of self-reinforced silicon nitride, J. Am. Ceram. Soc. 76 (11) (1993) 2737.
[5] P.L. Chen, I.W. Chen, In situ alumina–alumina platelet composite, J. Am. Ceram. Soc. 75 (9) (1992) 2610.
[6] L. An, H.M. Chan, R-curve behavior of in situ toughened Al_2O_3:$CaAl_{12}O_{19}$ ceramic composites, J. Am. Ceram. Soc. 79 (12) (1996) 3142.
[7] N. Iyi, S. Takegawa, S. Kimura, The crystal chemistry of hexaluminates: β-alumina in α-alumina ceramics, J. Solid State Chem. 83 (1989) 8.
[8] M.K. Cinibulk, Microstructure and mechanical peoprerties of a hibonite interface in alumina-based composites, Ceram. Eng. Sci. Proc. 16 (5) (1995) 633.
[9] L. An, H.M. Chan, N.P. Padture, B.R. Lawn, Damage resistance alumina-based layer composites, J. Mater. Res. 11 (1996) 204.
[10] L. An, H.M. Chan, K.K. Soni, Control of calcium hexaluminate grain morphology in in situ toughened ceramics composites, J. Mater. Sci. 31 (1996) 3223.